

Effects of second-order hydrodynamics on the efficiency of a wave energy array

H.A. Wolgamot^{a,*}, R. Eatock Taylor^b, P.H. Taylor^b

^a*University of Western Australia 35 Stirling Highway, CRAWLEY WA 6009, Australia*

^b*Dept of Engineering Science, University of Oxford Parks Road, Oxford OX1 3PJ, United Kingdom*

Abstract

This paper considers power absorption by a square array of four heaving truncated cylinders subject to monochromatic incident waves, where the hydrodynamic calculations are correct to second-order. This idealised WEC array is of particular interest as it supports a near-trapped mode which offers the opportunity for strong hydrodynamic interactions between WECs. However, for typical WEC geometries this mode can only be excited at second-order. The approach taken is to seek to maximise the significance of the second-order effects, though even in a rather extreme case (a near-trapped mode in shallow water) the maximum additional power is approximately 30% of the linear power, while in all other cases the additional power is much smaller.

Keywords: wave energy, second-order, nonlinearity, array, near-trapping

1. Introduction

A large body of work has been carried out analysing wave energy converters (WECs) using linear potential flow theory (see, for example, [1]). Fewer attempts have been made to use second-order potential flow methods to analyse wave energy devices. Mavrakos et al [2] analysed a single heaving truncated cylinder WEC both with and without a toroidal structure surrounding it. Calculations of first and second-order loads were used to calculate absorbed power, though the semi-analytical matched eigenfunction expansion method used was only applicable to fixed structures at second-order (though fixed and moving structures at first-order). The effect of the second-order forces was found to be very small, though most significant for long waves in shallow water, where the second order incident potential is larger. Bellew and Stallard [3] considered second-order forces on a 2-device array of hemispheres in irregular waves and

*Corresponding author

Email addresses: hugh.wolgamot@uwa.edu.au (H.A. Wolgamot),
r.eatocktaylor@eng.ox.ac.uk (R. Eatock Taylor), paul.taylor@eng.ox.ac.uk (P.H. Taylor)

found the second-order forces to be small. In contrast Nader et al [4] found that second-order effects could become significant in an Oscillating Water Column (OWC) WEC.

The interaction of second-order incident waves and fixed structures has been addressed by a number of authors. Different methods of calculating the second-order force on an isolated fixed cylinder were developed [5, 6, 7]. The problem of second-order wave diffraction by a square four-column array of bottom mounted cylinders was studied by Malenica et al [8] using a semi-analytical method. For such arrays they reported significant modifications (increases) of the forces on the cylinders in the array when compared to linear theory. Furthermore, with access to the free surface motions they were able to report near-trapping of the second-order waves, manifested in the form of large free surface elevations, at second-order frequencies equal to the known linear near-trapping frequencies for this problem [9]. The influence of these near trapped modes when excited at second-order has been emphasised in subsequent studies [10, 11].

Applications of second-order potential flow theory to the moving body problem have been less common. The sum frequency forces on a freely floating hemisphere in bichromatic waves were investigated by Kim and Yue [12]. They found that the second-order term due to first order body motions was significant, though in general the relative phases of the various second-order terms lead to the total second-order force being relatively modest. First- and second-order heave, pitch and surge motions of a freely floating truncated cylinder in monochromatic waves were investigated by Zaraphonitis and Papanikolaou [13]. They noted that the second-order responses in this case had multiple resonant peaks due to interaction between first-order terms. Further investigations of moving bodies at second order have been conducted [14, 15, 16].

This paper considers power absorption by an array of four generic heaving WECs in monochromatic waves, in a square arrangement which can support a near-trapped mode. Power absorption by the array due to both first- and second-order excitation is considered, where the second-order forces are determined using a full moving-body formulation. With low water depth and where the near-trapped mode is excited this represents a situation in which maximal second-order power absorption might be expected.

2. Theory

2.1. Incident waves

In a potential flow formulation the governing equation for the velocity potential Φ is the Laplace equation

$$\nabla^2 \Phi = 0 \tag{1}$$

which applies throughout the fluid. Although this governing equation is linear the free surface boundary conditions are nonlinear so a perturbation analysis is introduced and the velocity potential (and free surface elevation) are expressed

in terms of a power series in terms of the small parameter ϵ (where $\epsilon \ll 1$ is equal to the wave slope kA) such that:

$$\Phi = \epsilon \Phi^{(1)} + \epsilon^2 \Phi^{(2)} + \dots \quad (2)$$

The first- and second-order velocity potentials for the incident waves are then written as

$$\epsilon^m \Phi_I^{(m)} = \text{Re}\{\phi_I^{(m)} e^{-im\omega t}\} \quad (3)$$

where m is 1 or 2 and

$$\phi_I^{(1)} = \frac{-igA}{\omega} \frac{\cosh k(z+h)}{\cosh kh} e^{ikx} \quad (4)$$

while

$$\phi_I^{(2)} = \frac{-3i\omega A^2}{8} \frac{\cosh 2k(z+h)}{\sinh^4 kh} e^{2ikx}. \quad (5)$$

This second-order velocity potential is associated with a free surface profile with half the wavelength of the linear wave, leading to a complete free surface profile with flatter troughs and steeper crests (note that the second-order wave travels at the same speed as the linear wave). In deep water ($kh \rightarrow \infty$) the second-order incident potential vanishes, though the double frequency contribution to the free surface does not.

For the perturbation approach to be valid the second order terms must be small relative to the first order terms - in deep water this is true provided kA is small, as been assumed previously. In shallow water the depth becomes important and second-order theory may be applied only up to the limit given by the Ursell parameter

$$\frac{A/h}{(kh)^2} \lesssim \frac{1}{3} \quad (6)$$

beyond which cnoidal wave theory is more appropriate [17].

The wave power transported by the linear incident wave per unit width of wave front is [1]

$$J = \frac{\rho g^2 D(kh)}{4\omega} A^2 \quad (7)$$

where

$$D(kh) = \left\{1 + \frac{2kh}{\sinh 2kh}\right\} \tanh kh. \quad (8)$$

is a depth function which is unity in deep water.

2.2. DIFFRACT

Hydrodynamic calculations in this paper are performed with the boundary element code DIFFRACT [18]. DIFFRACT has been extended to compute forces on multiple moving bodies at second-order - details of the formulation are given in [19]. WEC (translational) velocities are computed at each order, m , according to

$$\{-mi\omega(\mathbf{M} + \mathbf{A}) + \mathbf{B} + \mathbf{D} - i\frac{\mathbf{C}}{m\omega}\}\hat{\mathbf{u}}^{(m)} = \hat{\mathbf{F}}^{(m)} \quad (9)$$

Table 1: Second-order heave forces on a freely floating hemisphere, non-dimensionalised by $\rho g a A_i A_j$ where a is the radius and $A_{i,j}$ the respective wave amplitudes.

$(\omega_i^2 a/g, \omega_j^2 a/g)$	Source	Total	$F_Q^{(2)}$	$F_{BB}^{(2)}$	$F_P^{(2)}$
(1.2,1.2)	KY	2.338	2.085	3.219	1.204
	DIFF	2.332	2.150	3.269	1.213
(1.2,1.4)	KY	1.866	1.200	2.034	1.134
	DIFF	1.866	1.237	2.064	1.140
(1.4,1.4)	KY	1.516	0.720	1.254	1.142
	DIFF	1.557	0.740	1.294	1.194

where the force at first-order $\hat{F}^{(1)}$ is the (complex amplitude of the) linear exciting force but at second-order $\hat{F}^{(2)}$ includes terms due to products of first-order terms as well as those due to the second-order incident wave. Hence the force at second-order depends upon the first-order motions, and therefore on the choice of power take-off coefficients. The terms \mathbf{M} , \mathbf{A} , \mathbf{B} and \mathbf{C} are the matrices of mass, hydrodynamic added mass, radiation damping and hydrostatic stiffness, while \mathbf{D} is a (diagonal) matrix of applied linear mechanical damping (representing simple power take-off). Note that the radiation damping and added mass are computed using identical expressions at first- and second-order as in the standard second-order decomposition.

For linear calculations in DIFFRACT the submerged body surfaces and inner water planes of the bodies must be meshed with quadratic elements. For second-order calculations the free surface must be meshed out to some radius, beyond which various asymptotic methods are used. To achieve converged second-order results it is critical that the mesh be small enough to resolve the high-frequency waves (i.e. several elements per wavelength) while the outer meshed radius must also be far enough from the body for the evanescent modes to have decayed.

Verification of DIFFRACT against the semi-analytical solution of [8] for a square array of four bottom-mounted circular cylinders is available in the literature [10]. For second-order forces on moving bodies, DIFFRACT is here compared to Kim and Yue [12], who examined the second-order forces on a freely floating hemisphere. A comparison between the results of Kim and Yue (KY) and the current implementation of DIFFRACT (DIFF) is given in Table 1 for the heave forces on the moving hemisphere, for the limited set of frequency pairs composed of deep-water wavenumbers 1.2 and 1.4. In these tables $F_Q^{(2)}$, $F_{BB}^{(2)}$ and $F_P^{(2)}$ are as defined in [12].

Note that due to the hemispherical geometry, rotational modes have no effect in this case. For general bodies rotational modes may introduce substantial additional complexity. In this paper we consider power absorption in cases where each body can move in a single translational mode (heave) only and hence the comparison to Kim and Yue is sufficient. Extending the analysis to include rotational modes may be expected to be more complicated, and further

validation would need to be pursued. Conceptually, however, it is considered that including only translational modes may be sufficient to provide some insight into second-order behaviour, and is also in accordance with the way some of these WECs operate.

To provide further confidence in the use of DIFFRACT for second-order calculations involving moving bodies, results from DIFFRACT have been compared with results from the fully nonlinear potential flow code OXPOT [20]. Comparisons were made for a limited set of single cylinders in regular waves, restricted to move in heave only. One case is shown in Fig. 1 - the second-order heave displacement of a single cylinder of radius 10m and draft 20m in incident regular waves of period 15 seconds and amplitude 1m. Encouraging agreement between the two independent methods is observed.

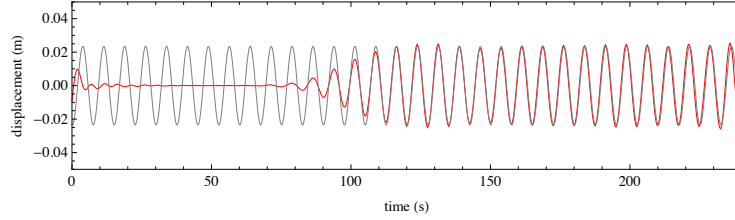


Figure 1: second-order heave displacement of a single truncated cylinder ($d=20\text{m}$, $a=10\text{m}$) in regular waves with $T = 15$ seconds. The steady-state harmonic signal is from DIFFRACT, while the signal with an initial transient is from the fully nonlinear potential flow code OXPOT.

2.3. Aspects of power calculations with second-order hydrodynamics

When second-order forcing is included in the analysis of arrays of wave energy devices in monochromatic waves there are forces and responses at two distinct frequencies, ω and 2ω . A general derivation of the time-average power delivered by a force and velocity, both harmonic with frequency ω , is given by [1], equation 2.77. For the case where the force F and velocity u are expressed in a perturbation expansion and have components at two frequencies, ω and 2ω , the calculation may be extended to the following:

$$\begin{aligned}
P(t) &= F(t)u(t) \\
&= (\epsilon F^{(1)}(t) + \epsilon^2 F^{(2)}(t))(\epsilon u^{(1)}(t) + \epsilon^2 u^{(2)}(t)) \\
&= \frac{1}{2}(\epsilon \hat{F}^{(1)} e^{-i\omega t} + \epsilon \hat{F}^{(1)*} e^{i\omega t} + \epsilon^2 \hat{F}^{(2)} e^{-2i\omega t} + \epsilon^2 \hat{F}^{(2)*} e^{2i\omega t}) \times \\
&\quad \frac{1}{2}(\epsilon \hat{u}^{(1)} e^{-i\omega t} + \epsilon \hat{u}^{(1)*} e^{i\omega t} + \epsilon^2 \hat{u}^{(2)} e^{-2i\omega t} + \epsilon^2 \hat{u}^{(2)*} e^{2i\omega t}) \\
&= \frac{1}{4}(\epsilon^2 \hat{F}^{(1)} \hat{u}^{(1)} e^{-2i\omega t} + \epsilon^2 \hat{F}^{(1)} \hat{u}^{(1)*} + \epsilon^3 \hat{F}^{(1)} \hat{u}^{(2)} e^{-3i\omega t} + \dots)
\end{aligned}$$

where the full expansion is omitted. In the time averaged power the sinusoidal terms vanish so that the mean power (denoted by an overbar) may be expressed

as

$$\begin{aligned}\overline{P(t)} &= \frac{1}{4}(\epsilon^2 \hat{F}^{(1)} \hat{u}^{(1)*} + \epsilon^2 \hat{F}^{(1)*} \hat{u}^{(1)} + \epsilon^4 \hat{F}^{(2)} \hat{u}^{(2)*} + \epsilon^4 \hat{F}^{(2)*} \hat{u}^{(2)}) \\ &= \frac{1}{2} \epsilon^2 \text{Re}\{\hat{F}^{(1)} \hat{u}^{(1)*}\} + \frac{1}{2} \epsilon^4 \text{Re}\{\hat{F}^{(2)} \hat{u}^{(2)*}\}\end{aligned}\quad (10)$$

indicating that, as expected, there is no cross-coupling between the linear and double frequency harmonics. There is a power due to the linear terms, which is proportional to the square of the wave amplitude and is identical to the expression obtained without the second-order case; and a term due to the second-order force and response, which is proportional to the fourth power in the wave amplitude.

If the case of incident irregular waves is considered it is apparent that similarly there is, in general, no mean coupling between the first- and second-order signals. However, more detailed consideration of one case is required: coupling between the linear force (or response) at frequency ω and the second-order response (or force) at frequency ω (due to incident wave pairs with frequencies which sum to this value). In this case, according to the argument above, it is possible in principle for a mean power term (proportional to wave amplitude cubed) to exist due to these frequency components. If this were to occur it would dominate the power term proportional to wave amplitude to the fourth power, and mark a serious deficiency in a monochromatic analysis (in which this effect could not be included). However, it is important to realise that in any realisation of a random sea, the phases of each component are randomly distributed, such that, averaged over all possible realisations of a particular sea-state, this third-order power term would be zero.

In a similar vein, given that wave-structure interaction is a fully nonlinear phenomenon, higher order terms should be considered. In particular, power cannot be calculated correct to the fourth power in wave amplitude without considering coupling between linear and third-order signals. This possibility arises because third order terms would be present at ω and 3ω , and would be correlated with the linear term at frequency ω (evidently only the third order term at ω could contribute to time-average power). This is true both in the incident field and for the power absorbed by the WEC. Using DIFFRACT, which extends only to second-order, it is impossible to quantify the third-order effect, and this potential contribution to power is therefore neglected.

There is an issue of terminology here, since the power due to the first-order terms is proportional to the square of the wave amplitude and the power due to the second-order terms is proportional to the fourth power. In this paper the terms ‘linear power’ and ‘second-order power’ will be taken to mean these two power terms, respectively.

3. Linear analysis of array

An array of bottom-mounted cylinders of radius a laid out in a square arrangement with centre-to-centre spacing $4a$ was one configuration investigated

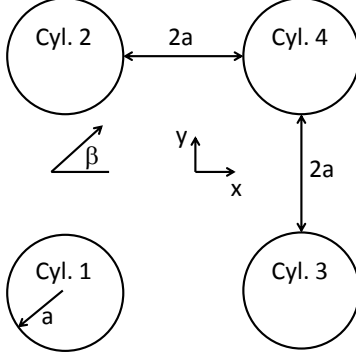


Figure 2: Layout of four cylinder array.

by Evans and Porter [9] (shown in Fig. 2). The lowest-frequency near-trapped mode for this geometry occurs when the linear near-trapping wavelength is approximately equal to the centre-to-centre spacing, and is present also for an array of truncated cylinders [21]. At full scale the near-trapped mode is likely to have a significant effect only if it coincides in frequency with a reasonable fraction of the incident wave energy. Babarit et al [22] presented statistics for five wave energy test locations along the west European coast, and the peaks in the scatter diagrams occurred for peak periods in the range 7 to 11 seconds. Thus a typical value of the monochromatic wave period, T , of 9 seconds is adopted for the purposes of this paper.

For such a wave to coincide with the near-trapped mode the WECs must be very large - for a wave with period 9 seconds in deep water the wavelength is 126m, meaning that the WECs would have to have a radius of around 30m. If the near trapping is excited at second-order, however, the incident ka value could be much smaller, with the shorter-wavelength second-order free wave component exciting the near-trapped mode. In this paper the WECs will be chosen to have a radius of 8m - this falls within the range of typical dimensions for such devices, identified by Babarit [23] as being (diameter) 10-20m. With this radius an incident wave of period approximately 9 seconds in 32m deep water will excite the near-trapped mode at second-order. The near-trapped mode will only be excited by waves incident along an array diagonal ($\beta = 45^\circ$ in Fig. 2), so only this incident wave direction will be considered in this paper.

3.1. Linear power absorption

Before considering second-order analysis it is important to understand something about the array's performance using linear theory. It is well known that optimum (linear) power absorption for any array may be determined from

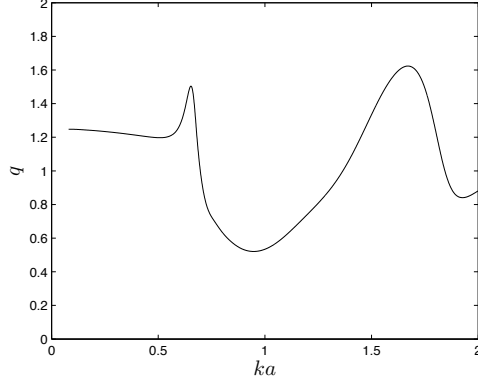


Figure 3: Interaction factor for deep draft 4 cylinder array in heave, waves incident along a diagonal of the array.

knowledge of the exciting force and damping coefficients, according to the expression [24, 25]:

$$P_{MAX,N} = \frac{1}{8} \mathbf{F}_e^\dagger \mathbf{B}^{-1} \mathbf{F}_e \quad (11)$$

where \mathbf{F}_e is the vector of exciting forces and \mathbf{B} the matrix of damping coefficients. This maximum power may be used to form an interaction factor, q , by dividing by the optimum performance of the devices in isolation.

It is found that the optimum interaction factor for power absorption by the array analysed by [21] (Fig. 2 with draft $2a$) in heave, with waves incident at $\beta = 45^\circ$, is as given in Fig. 3 (obtained here using DIFFRACT). It is evident that there are two zones of beneficial interaction - a narrow peak at around $ka = 0.65$ and a much broader peak around the near-trapping wavenumber at $ka = 1.66$. For this array $ka = 0.65$ is close to the frequency of the near-wave-free mode identified by Siddorn and Eatock Taylor [21] and analysed in more detail by Wolgamot et al [26]. This near-wave-free mode was found to be associated with motion of the four cylinders as a rigid body in heave. This is clearly illustrated by using the special symmetry of this array to adopt a change of basis (as in [26]), where the power absorbed in each body motion mode (corresponding to the eigenvectors of the damping matrix) is shown in Fig. 4. The modes labelled in the legend of this figure follow the cylinder numbering in Fig. 2, where $[1 \ 1 \ 1 \ 1]$ is the rigid body motion mode and it is noted that due to the symmetry of the array the eigenvector $[1 \ 1 \ -1 \ -1]$ is repeated. The peak in absorbed power due to the near-wave-free mode around $ka = 0.65$ is therefore of little interest as a near-wave-free mode also corresponds to very small exciting force (by the Haskind relations, e.g. [27]) and so large power absorption must be associated with extremely large (and unphysical) displacements. (The peak is due to the fact that for this incident wave direction the exciting force is less dramatically reduced than the damping; the reverse is true for $\beta = 0$.) Hence the only peak of real interest is that due to the near-trapped mode.

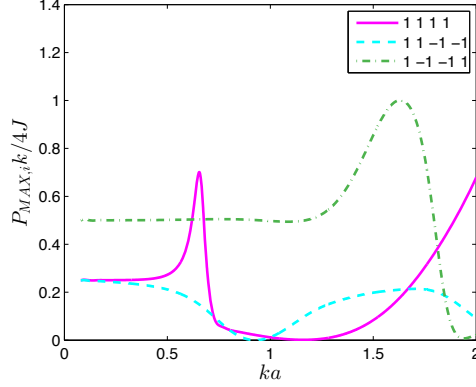


Figure 4: Normalised maximum power absorbed in each body motion mode identified in the legend, for waves incident from $\beta = 45^\circ$. Due to symmetry the second mode is repeated.

3.2. Power take-off

Different methods of power take-off and control for wave energy devices exist. Satisfying the optimum condition (11) corresponds (in general) to reactive control, i.e. at each frequency the mechanical impedance is selected such that the optimum condition is satisfied and there is a reactive power flow. This corresponds to each device oscillating with optimum amplitude and phase.

It is also possible to control an array using only resistive, or passive, control. For a single heaving body without any control of the phase (e.g. mechanical stiffness) an expression for the mechanical damping which leads to optimum power absorption is given in equation 3.40 of [1]. Since the phase is not controlled this is a fairly weak optimisation. An extension of this method to arrays was pursued by Bellew et al [28], who implemented resistive control for a 5 hemisphere array by using the optimum condition with matrices in place of the appropriate scalars for the single degree of freedom system. As this results in a dense matrix they also implemented a mechanical damping matrix equal to the diagonal of the matrix described above. This method was found to give results close to strategies where the damping values for each hemisphere were selected based on an optimisation procedure, except near resonance where the optimised values lead to slightly more absorbed power.

In the case of the four cylinder arrays being considered in this paper, the symmetry of the array means that implementing the method of [28] leads to the same damping value for each cylinder. In fact, there is little difference between the power absorbed using the damping for a single cylinder in isolation, or the matrix method of [28]. No distinction will therefore be made between these methods and the approach will be referred to as optimal resistive control.

4. Power from near trapped mode at second-order

In the works on second-order power absorption by rigid bodies undertaken to date the power due to second-order forcing has been found to be small. The studies of Mavrakos et al [2, 29] investigated a single shallow draft cylinder in shallow water and found that including second-order hydrodynamics led to an additional power absorption of approximately 10%. This was found to be the case when the cylinder was controlled using resistive control only, and when a nonlinear power take-off (PTO) was applied. This is a fairly small increase in absorbed power, and it was stated that other cases had been tested in which the absorbed power was substantially smaller - i.e. insignificant.

In the other study of second-order effects on wave energy devices, Bellew et al [3, 30] computed only the forces on a 2×1 array of hemispheres in irregular waves. When the forces at a single component frequency due to first- and second-order potentials were compared it was found that over most of the frequency range the second-order forces were less than 10% of the first-order forces, though the second-order forces could exceed this limit at high and low frequencies. The absorbed power was not calculated, but since the absorbed power is crudely proportional to the square of the force (the PTO characteristics also have a large influence) at a single frequency the absorbed power due to second-order effects would be expected to be much smaller than the first-order power. If the integrated effect over the spectrum is then considered it may be seen that the additional power due to second-order forcing may be expected to be much smaller than that due to the first-order forcing. The work of [4] on OWCs, however, suggested that it is possible for resonant phenomena at second-order to be important for power absorption.

In light of the results summarised above, the approach taken in this paper is to seek to maximise the second-order power, and to thus evaluate whether, even in relatively unrealistic cases, second-order effects may become significant. Hence second-order effects are only calculated here in monochromatic waves. This is consistent with the approach above, as interactions in arrays of wave energy devices at first-order, and fixed structures at second-order, indicate that interaction effects are weakened in irregular waves (e.g. [10, 31]). Note that when power due to first- and second-order forcing is compared, the comparison will therefore be between the power due to forces and responses at ω and those at 2ω . Further, resistive damping will be employed for power take-off, as implemented by [29]. In this case the power take-off will be weakly optimised for the first-order hydrodynamics, but while it would be possible to optimise more strongly in regular waves, this would tend to favour the power due to the linear terms over the power due to the second-order terms. While this may increase total power it is not the approach taken here.

In this paper the behaviour of two different four cylinder arrays subject to incident monochromatic waves will be considered. The cylinders in each array will be considered to be free to respond (independently) in heave only. Only waves incident along the diagonal of the array, equivalent to $\beta = 45^\circ$ in Fig. 2 will be considered. The results will be presented at full scale, so

that the relative importance of the first- and second-order effects may be easily grasped. To dimensionalise the results a moderately large wave amplitude of 2m will be used for all frequencies to try to maximise the second-order effects - evidently using the same amplitude means that waves at high frequency are steeper than at low frequency. (For a wave of period 9 seconds and amplitude 2m, the steepness kA is equal to 0.1.) Results will be plotted against both nondimensional wavenumber ka , and period, T .

4.1. Deep draft case

Initially a deep draft case, a scaled version of the array considered in the linear calculations above, will be considered. With device radius 8m this corresponds to a draft of 16m, water depth of 32m and centre-to-centre spacing of 32m. A range of incident wave periods from 5 to 15 seconds will be considered, corresponding to a range of non-dimensional wavenumbers $0.21 < ka < 1.29$ in this water depth. The near-trapped mode is expected to occur at approximately $ka = 1.66$, such that it will not be excited at first-order; this mode may, however, be excited at second-order when the incident wave has wavenumber $ka = 0.44$ and period 8.8 seconds. The heave motion resonance for these cylinders is satisfied at approximately $ka = 0.42$. The cylinders are assigned identical damping values, selected using optimal resistive control at each frequency. In all cases the mesh used in DIFFRACT has been selected based on experience as one which will give converged values, and then checked with different mesh spacings and radii of the discretised outer free surface at the low and high frequency ends of the range and at selected intermediate frequencies. In all cases satisfactory convergence was observed.

Fig. 5 displays the heave forces on the four cylinders (with three lines shown due to the symmetry associated with the chosen wave heading). The first-order force, second-order force on the moving body, and second-order force on a fixed body are shown, with the forces plotted against the incident linear wavenumber such that the second-order forces actually occur at twice the indicated frequency. It is apparent that the forcing due to the first-order motions has created a large peak in the second-order forces around the resonant frequency - that this is not due to near-trapping may be seen by comparing the second-order fixed and moving body results. In fact, the near-trapped mode appears to have little influence on the second-order heave forces in this configuration. The effect of the near-trapped mode may be seen in Fig. 6 which shows the first-order, second-order fixed body and second-order moving body surge forces on the array. It is apparent that the heave resonance has a noticeable effect on the second-order surge force when the body is moving, but there is also an effect of similar size in the fixed body case, at the near trapping frequency. At the higher end of the frequency range, the second-order heave force becomes comparable to, or greater than, the first-order force. As the waves are steepest in this range (as discussed above) and considering the slow depth attenuation of the second-order scattered potential (e.g. [32]) this is unsurprising.

The heave forces may be used to calculate the second-order motions of the cylinders according to Eq. (9), and hence the power absorbed by the array.

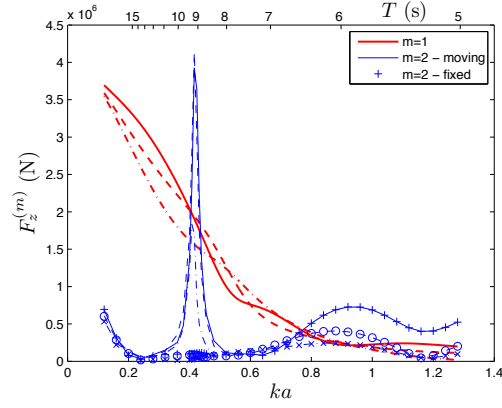


Figure 5: Heave forces on four cylinder deep draft array for incident wave of amplitude 2m. For first- and second-order moving body forces the full, dashed and dash-dotted lines represent the front, middle and rear cylinders, respectively. For the second-order fixed body case the +, o and x labels apply respectively.

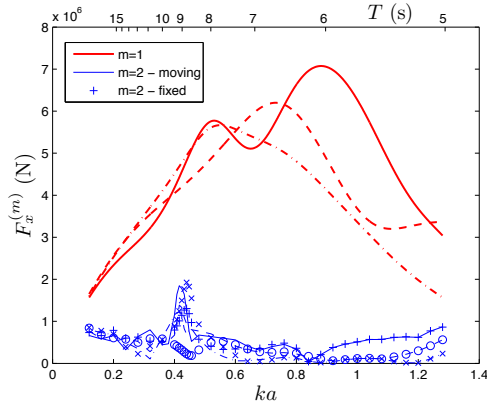


Figure 6: Surge forces on four cylinder deep draft array. Symbols are as in Fig. 5.

Fig. 7 displays the absorbed power and Fig. 8 the heave excursions (on logarithmic axes!). A relatively deep-draft cylinder like those being considered here has a relatively high resonant response but a low bandwidth, and this may be seen in both curves. The second-order power and response around the peak is insignificant in comparison to the peak power/displacement. It is apparent that the second-order power becomes comparable to the linear power only at high frequencies when the linear power is very low. For this array, the additional power absorbed due to second-order effects is insignificant.

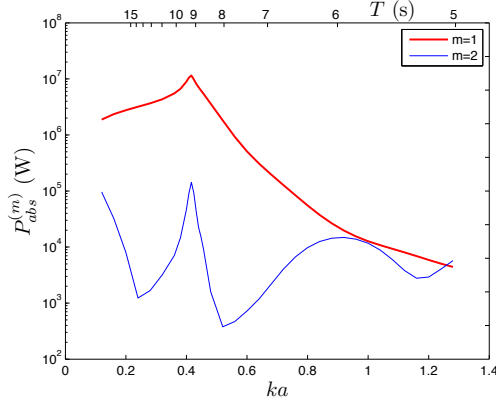


Figure 7: Power absorbed by four cylinder deep draft array.

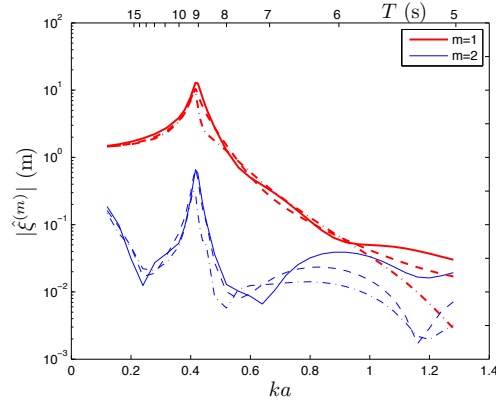


Figure 8: Displacements of four cylinder deep draft array.

Evidently, the excursion amplitudes shown in Fig. 8 become very large around resonance. Displacements peak at around 12m, or 6 times the incident wave amplitude. This is larger than, for example, the limiting value of the device radius for which linear theory was found to work well by [33]. With a weakly nonlinear model, the range in which the theory could be expected to

give accurate results for a moving body is not known. However, for practical reasons, it is often desirable to limit the amplitude of motion of the device. Hence the second-order heave force on the body when it is able to move up to a limit of twice the incident wave amplitude (4m) is shown in Fig. 9. For these calculations the amplitude has been limited by increasing the damping coefficient for each body until the largest amplitude falls below the limit. Evidently this restriction makes a significant difference to the second-order heave force around resonance, though the conclusion that the second-order force leads to negligible additional power is unchanged.

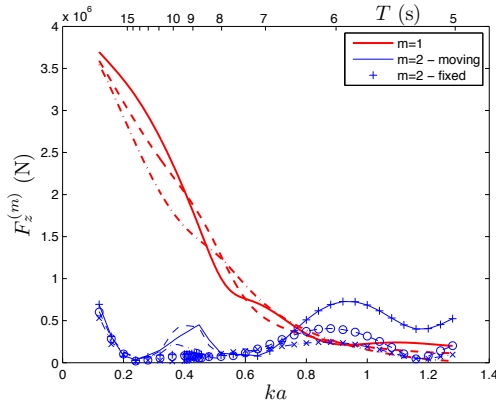


Figure 9: Heave forces on four cylinder deep draft array for incident wave of amplitude 2m, with first-order displacements limited to 4m. Symbols are as in Fig. 5.

4.2. Shallow draft case

The additional power absorbed due to second-order forcing of the array of deep draft cylinders considered in the previous section was found to be insignificant. Mavrakos et al [29] found 10% increases in absorbed power from a single cylinder due to the inclusion of second-order effects when shallow water was considered - i.e. close to the Ursell limit given in Eq. (6). It is therefore desirable to investigate the present array, where body motions are considered and a near-trapped mode exists, in similar conditions. For this purpose, a water depth of 11m has been selected. With this choice, the range of wave periods from 5 to 15 seconds corresponds to a wavenumber range of $0.33 < ka < 1.35$.

To reduce the water depth it is also necessary to reduce the draft of the cylinders - a reduction of the draft by a factor of 4, to 4m, was selected as convenient for this case. This draft reduction may also result in higher heave forces on the cylinders at high frequency, due to the depth attenuation of the wave-induced pressure. According to linear theory, reducing the draft will lead to higher heave forces at the near-trapped mode frequency. At second-order, however, the effect may be different as the second-order scattered potential decays slowly with depth. Newman [7] considered a bottom mounted cylinder

and noted that the depth is of primary importance when the wavelength is large relative to the depth, while at high frequency the slow depth decay of the second-order potential is more significant, suggesting that draft may be more important at high frequency. The heave forces on a limited range of fixed truncated circular cylinders spanning the space between the deep draft case considered above and the shallow draft case considered in this section are shown in Fig. 10. As in previous cases, the wavenumber on the horizontal axis is the wavenumber of the first-order incident wave. Noting that the near-trapped mode is at approximately $ka = 0.5$, it may be seen that reduction of the cylinder draft without changing the water depth does not increase the second-order heave force on the cylinder around this frequency - in fact, the force may be reduced. At these frequencies, it is only when the depth is substantially reduced that an increase in force is noticed. At high frequencies there is an increase in the heave force for decreasing draft and water depth, but these frequencies are outside the range considered in the current investigation.

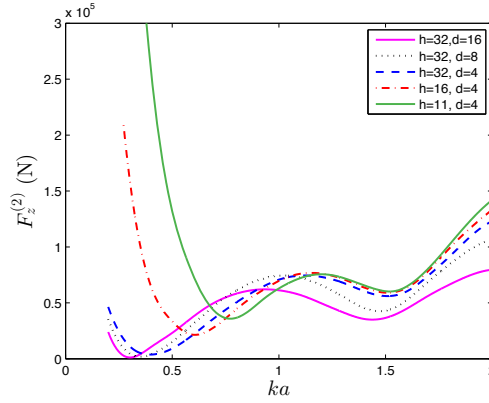


Figure 10: Second-order heave forces on a range of isolated, fixed truncated cylinders with radius $a = 8m$ and draft, d , and depth, h , values varying between the deep draft and shallow draft cases. The ka axis is the wavenumber of the linear incident wave.

Returning to the shallow draft array case, the near-trapped mode may be excited by a linear incident wave at approximately $ka = 1.7$, and can therefore be excited at second-order by an incident wave with wavenumber $ka = 0.61$, or period 8.8 seconds. The heave resonance for a single cylinder of this geometry occurs at $ka = 1.1$, or incident wave period 5.7 seconds. Due to the differing dimensions this cylinder would be expected to have a lower peak power absorption but higher bandwidth, with a lower peak response, relative to the deep draft cylinder in the previous section. This difference is apparent in Fig. 11 in which the heave forces on the cylinders in the array at first- and second-order are shown. There is now a substantial peak in the second-order force at the near-trapping frequency, but no feature around the heave resonance, in contrast to the deep draft case. The second-order forces on the array when the cylinders are fixed is shown, and it is apparent that the forces differ from the forces on

the moving cylinders across the frequency range. It is interesting to note that the peak in the heave force when the near-trapped mode is excited at second-order is higher for the moving body than for the fixed body case. The thick black line indicates the Ursell limit Eq. (6), below which second-order theory is no longer valid for the given incident wave amplitude. This results from the desire to choose parameters for this array for which the near-trapped frequency was close to the Ursell limit - after the cylinder draft was chosen (with wave amplitude unchanged from Section 4.1), the water depth of 11m was found to satisfy this aim. Evidently, longer waves must therefore exceed the limit unless the amplitude is reduced.

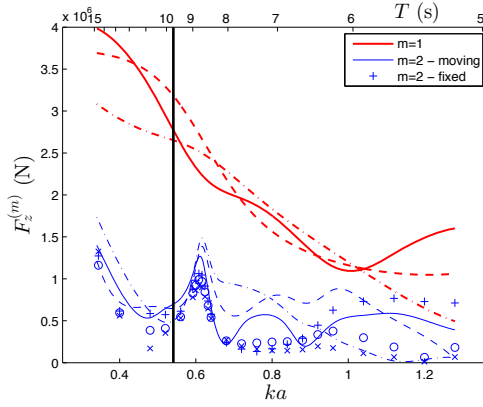


Figure 11: Heave forces on four cylinder shallow draft array for incident wave of amplitude 2m. For first- and second-order moving body forces the full, dashed and dash-dotted lines represent the front, middle and rear cylinders, respectively. For the second-order fixed body case the +, o and x labels apply respectively. The dark line represents the Ursell limit (6).

Using these forces, the cylinder responses and absorbed power at first- and second-order were calculated and are shown in Figures 12 and 13 respectively. The first-order excursion amplitudes in Fig. 12 differ substantially from those in Fig. 8 and are relatively constant, and moderate, across the frequency range of interest. At second-order, there is a peak at the near-trapped mode frequency. The absorbed power in Fig. 13 has one very noticeable feature at the near-trapping frequency. At the peak, the second-order power is approximately 31% of the first-order power contribution, which is the maximum ratio attained over the frequency range considered. Outside the narrow frequency band in which the near-trapped mode may be excited, the second-order power is a much smaller fraction of the first-order power. There is a range of frequencies, approximately $0.65 < ka < 0.85$, where the second-order power is between 5-10% of the first-order power - outside of this range the second-order power is even less significant.

A final comparison of interest is to plot a modified (sub-optimal) interaction factor q_{so} for the array, at first- and second-order. This is the ratio of the power absorbed by the array (at the appropriate order) to the power absorbed by four isolated cylinders with the same power take-off, and is displayed in Fig. 14.

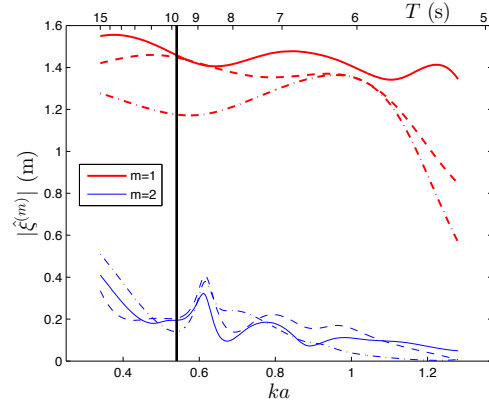


Figure 12: Amplitude of heave displacements for shallow draft array. For first- and second-order displacements the full, dashed and dash-dotted lines represent the front, middle and rear cylinders, respectively.

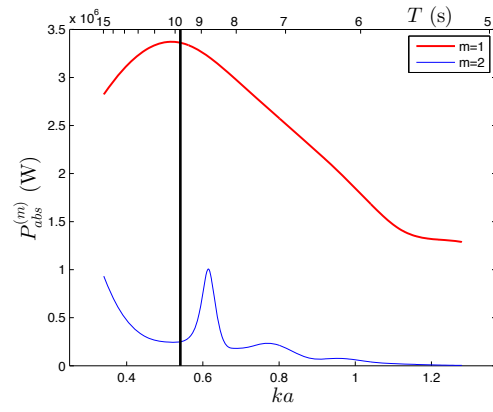


Figure 13: Power absorbed by heaving shallow draft array.

The linear interaction factor is less than one over most of the range, while the second-order interaction factor is much greater. For the linear case, this is in accord with Folley and Whittaker [34] who found that array interactions were minimal when resistive control was applied, since the radiated waves were small. The peak in the second-order interaction factor at the near-trapping frequency is matched by a broader peak at slightly higher frequency - for the broader peak the second-order force on a single cylinder is a local minimum, which amplifies the effect. Clearly the array interactions are relatively more important at second- than first-order, which is in agreement with Malenica et al [8] who found that the second-order force per cylinder on an array of fixed bottom mounted cylinders was greater than the force on an individual cylinder over a wide frequency range. Evidently interaction between WECs at second-order may occur more through the scattered than radiated waves, particularly when there is a near-trapped mode, which is why the conclusion of Folley and Whittaker does not seem to extend to second-order. However, it is again important to recognise that at all frequencies away from the near-trapped mode the second-order power from the array is less than 10% of the first-order power, and that the second-order power from a single cylinder at these frequencies is therefore even less important.

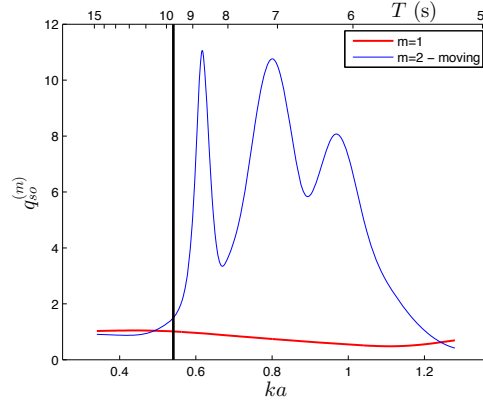


Figure 14: Sub-optimal interaction factor for first- and second-order power absorbed by shallow draft array with incident amplitude 2m.

Finally, it is well known (e.g. [10]) that the second-order free surface elevation at a near-trapped frequency may be large. It is therefore of interest to examine the free surface around the shallow draft array at the near-trapping frequency when the array is absorbing power. Hence the modulus of the first- and second-order free surface elevations are shown in Fig. 15 and Fig. 16 respectively. In the vicinity of the array the free surface due to the near-trapped mode dominates, and is extremely large (note that the amplitude of the second-order incident wave is only 0.6m). This contrast between the relatively modest power absorption at second-order and the extremely strong free surface effect indicates that even in a situation where the second-order effects are very large,

the second-order power is still relatively modest. Of course, the size of these free surface displacements calls into question the validity of the second-order theory in such shallow water, so that the second-order forces found here may in fact be overly large.

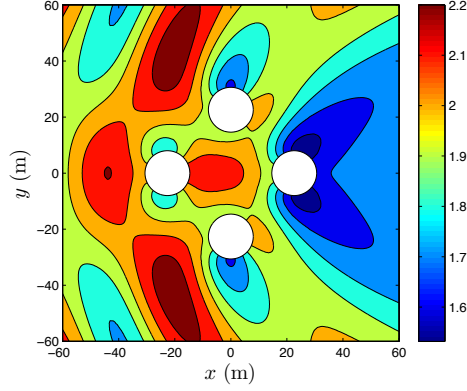


Figure 15: Maximum free surface elevation due to first-order incident, scattered and radiated waves around shallow draft array with optimal resistive control at $ka = 0.62$, for 2m incident wave. The colour axis is in metres.

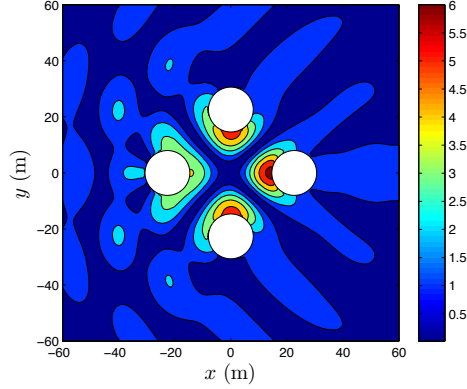


Figure 16: Maximum free surface elevation due to second-order scattered and radiated waves around shallow draft array with optimal resistive control at $ka = 0.62$, for 2m (linear) incident wave amplitude. The colour axis is in metres.

5. Conclusions

The forces, displacements and power absorption of two four cylinder arrays at first- and second-order have been calculated. Even in the most favourable

case, the second-order power was found to be only 31% of the first-order power, and this case represents a rather extreme situation as it:

- is at the Ursell limit
- is for a monochromatic wave
- involves quite closely spaced WECs
- involves an array which is rather weakly optimised at first-order
- excites a near-trapped mode with narrow bandwidth.

Away from this near-trapped mode the second-order power was found to be small, even when the second-order forces were relatively large. It appears that even weak optimisation of the mechanical power take-off system is sufficient to greatly favour the first-order response and absorbed power. When the first-order motions were significant (e.g. greater than a quarter of the incident wave amplitude) the second-order forces on the body calculated when the body was moving differed substantially from the forces calculated when the body was fixed, though the magnitude of the forces were similar and the overall conclusion about the significance of second-order power was thus relatively unaffected.

In light of all the other methods for optimising wave energy devices, seeking extra power from second-order effects seems to be a very unrewarding choice for deployment of further research effort. This may not be true for devices designed to always operate in shallow water, though other wave theories may also be more appropriate in very shallow near-shore regions. Of course, nonlinear effects may be much more significant for WECs in a survival context.

Acknowledgment

During the time this work was performed H.A. Wolgamot was supported by a University of Oxford Clarendon Fund Scholarship. The authors are grateful to Dr C.J. Fitzgerald for providing OXPOT simulation results for comparison purposes.

References

- [1] J. Falnes. *Ocean Waves and Oscillating Systems*. Cambridge University Press, 2002.
- [2] S. A. Mavrakos, G. M. Katsounis, and I. K. Chatjigeorgiou. Performance Characteristics of a Tightly Moored Piston-Like Wave Energy Converter Under First and Second-Order Wave Loads. In *Proceedings of the 27th International Conference on Offshore Mechanics and Arctic Engineering*, Estoril, Portugal, 2008. ASME.

- [3] S. Bellew and T. Stallard. Linear modelling of wave device arrays and comparison to experimental and second order models. In *International Workshop for Water Waves and Floating Bodies 2010*, 2010.
- [4] J.-R. Nader, S.-P. Zhu, and P. Cooper. On the efficiency of oscillating water column (OWC) devices in converting ocean wave energy to electricity under weakly nonlinear waves. In *ASME 2012 31st International Conference on Ocean, Offshore and Arctic Engineering*, pages 659–666. American Society of Mechanical Engineers, 2012.
- [5] D.L. Kriebel. Nonlinear wave interaction with a vertical circular cylinder. Part I: Diffraction theory. *Ocean Eng.*, 17(4):345–377, 1990.
- [6] F. P. Chau and R. Eatock Taylor. Second-order wave diffraction by a vertical cylinder. *J. Fluid Mech.*, 240:571–599, 1992.
- [7] J. N. Newman. The second-order wave force on a vertical cylinder. *J. Fluid Mech.*, 320:417–443, 1996.
- [8] S. Malenica, R. Eatock Taylor, and J. B. Huang. Second-order water wave diffraction by an array of vertical cylinders. *J. Fluid Mech.*, 390:349–373, 1999.
- [9] D. V. Evans and R. Porter. Near-trapping of waves by circular arrays of vertical cylinders. *Appl. Ocean Res.*, 19:83–99, 1997.
- [10] D. A. G. Walker, R. Eatock Taylor, P. H. Taylor, and J. Zang. Wave diffraction and near-trapping by a multi-column gravity-based structure. *Ocean Eng.*, 35:201–229, 2008.
- [11] J. R. Grice, P. H. Taylor, and R. Eatock Taylor. Second-order statistics and ‘designer’ waves for violent free-surface motion around multi-column structures. *Phil. Trans. Roy. Soc. A*, 373(2033):20140113, 2015.
- [12] M.-H. Kim and D.K.P. Yue. The complete second-order diffraction solution for an axisymmetric body Part 2. Bichromatic incident waves and body motions. *J. Fluid Mech.*, 211(1):557–593, 1990.
- [13] G.N. Zaraphonitis and A.D. Papanikolaou. Second-order theory and calculations of motions and loads of arbitrarily shaped 3D bodies in waves. *Marine structures*, 6(2):165–185, 1993.
- [14] W. I. Moubayed and A. N. Williams. The second-order diffraction loads and associated motions of a freely floating cylindrical body in regular waves: An eigenfunction expansion approach. *J. Fluids Struct.*, 8(4):417–451, 1994.
- [15] W.I. Moubayed and A.N. Williams. The sum-and difference-frequency wave loads and motions of a freely floating circular cylinder. *J. Fluids Struct.*, 9(3):323–355, 1995.

- [16] Y. Liu, D.K.P. Yue, and M.-H. Kim. First-and second-order responses of a floating toroidal structure in long-crested irregular seas. *Appl. Ocean Res.*, 15(3):155–167, 1993.
- [17] R. G. Dean and R. A. Dalrymple. *Water Wave Mechanics for Engineers and Scientists*. World Scientific., 1991.
- [18] F. P. Chau. *The second order velocity potential for diffraction of waves by fixed offshore structures*. PhD thesis, University College London, 1989.
- [19] L. Sun, R Eatock Taylor, and P. H. Taylor. Wave driven free surface motion in the gap between a tanker and an FLNG barge. *Appl. Ocean Res.*, 2015.
- [20] W. Bai and R. Eatock Taylor. Numerical simulation of fully nonlinear regular and focused wave diffraction around a vertical cylinder using domain decomposition. *Appl. Ocean Res.*, 29(1):55–71, 2007.
- [21] P. Siddorn and R. Eatock Taylor. Diffraction and independent radiation by an array of floating cylinders. *Ocean Eng.*, 35:1289–1303, 2008.
- [22] A. Babarit, J. Hals, M.J. Muliawan, A. Kurniawan, T. Moan, and J. Krokstad. Numerical benchmarking study of a selection of wave energy converters. *Renewable Energy*, 41:44–63, 2012.
- [23] A. Babarit. On the park effect in arrays of oscillating wave energy converters. *Renewable Energy*, 58:68–78, 2013.
- [24] D. V. Evans. Some analytic results for two- and three-dimensional wave-energy absorbers. In B.M. Count, editor, *Power from Sea Waves*, pages 213–249. Academic Press, 1980.
- [25] J. Falnes. Radiation impedance matrix and optimum power absorption for interacting oscillators in surface waves. *Appl. Ocean Res.*, 2(2):75–80, 1980.
- [26] H. A. Wolgamot, R. Eatock Taylor, and P. H. Taylor. Radiation, trapping and near-trapping in arrays of floating truncated cylinders. *J. Engng. Maths*, 91:17–35, 2015.
- [27] J. N. Newman. The interaction of stationary vessels with regular waves. In *Proceedings of the 11th Symposium on Naval Hydrodynamics*, pages 491–501, 1976.
- [28] S. Bellew, T. Stallard, and P.K. Stansby. Optimisation of a heterogeneous array of heaving bodies. In *Proceedings of the 8th European Wave and Tidal Energy Conference*, 2009.
- [29] S.A. Mavrakos, G.M. Katsaounis, and I.K. Chatjigeorgiou. Performance characteristics of tightly moored wave energy converters under first- and second- order wave loads. In *Proceedings of the 7th European Wave and Tidal Energy Conference*, 2007.

- [30] S.L. Bellew. *Investigation of the response of groups of wave energy devices*. PhD thesis, University of Manchester, 2011.
- [31] J. Cruz, R. Sykes, P. Siddorn, and R. Eatock Taylor. Wave farm design: Preliminary studies on the influences of wave climate, array layout and farm control. In *Proceedings of the 8th European Wave and Tidal Energy Conference*, 2009.
- [32] J.N. Newman. Second-harmonic wave diffraction at large depths. *J. Fluid Mech.*, 213(1):59–70, 1990.
- [33] J. Falnes and J. Hals. Heaving buoys, point absorbers and arrays. *Phil. Trans. Roy. Soc. A*, 370(1959):246–277, 2012.
- [34] M. Folley and T. J. T. Whittaker. The effect of sub-optimal control and the spectral wave climate on the performance of wave energy converter arrays. *Appl. Ocean Res.*, 31:260–266, 2009.